

Visible Light Responsive Titanium Dioxide (TiO₂) – a review

H.K. Shon¹, S. Phuntsho¹, Y. Okour¹, D.L. Cho², J.B. Kim^{2,3}, S. Na² and J.-H. Kim^{2,3*}

¹ Faculty of Engineering, University of Technology, Sydney, P.O. Box 123, Broadway, NSW 2007, Australia

² School of Applied Chemical Engineering & The Research Institute for Catalysis, Chonnam National University, Gwangju 500-757, Korea

³ Photo & Environmental Technology Co.Ltd., Gwangju 500-460, Korea

Abstract

Titanium dioxide (TiO₂) is one of the most researched semiconductor oxides that has revolutionised technologies in the field of environmental purification and energy generation. It has found extensive applications in heterogenous photocatalysis for removing organic pollutants from air and water and also in hydrogen production from photocatalytic water-splitting. Its use is popular because of its low cost, low toxicity, high chemical and thermal stability. But one of the critical limitations of TiO₂ as photocatalyst is its poor response to visible light. Several attempts have been made to modify the surface and electronic structures of TiO₂ to enhance its activity in the visible light region such as noble metal deposition, metal ion loading, cationic and anionic doping and sensitisation. Most of the results improved photocatalytic performance under visible light irradiation. This paper attempts to review and update some of the information on the TiO₂ photocatalytic technology and its accomplishment towards visible light region.

Keywords: visible light photocatalyst, titanium dioxide, semiconductor, TiO₂ modification

1 Introduction

TiO₂ semiconductor is the most popular photocatalyst because of its excellent optical and electronic properties, low cost, non toxicity, chemical and thermal stability [1]. TiO₂ has been used for environmental remediation purposes such as in the purification of water and air and also in the solar water splitting [2-7]. Photocatalysis is by far one of the most superior technologies in the environmental purification because unlike many other technologies, photocatalysis does not serve as a mere phase transfer but completely degrades the organic pollutants by converting to innocuous substances such as CO₂ and H₂O. Photocatalytic water-splitting using TiO₂ for hydrogen production provides a promising method to obtain clean, low-cost and environmentally friendly fuel by solar energy. Therefore the improvement and optimization of TiO₂ is an important task for heterogeneous photocatalysis in the future [8]. Many researches have been carried out not only to improve the photoactivity of TiO₂ under UV light but also to improve its activity under visible light region.

A number of scientific reviews have been published on visible light responsive (VLR) TiO₂ photocatalyst [9-15]. The above review papers mainly cover the recent

developments and progress of VLR TiO₂ in terms of photocatalytic water-splitting and degradation of organic pollutants. It also includes TiO₂ modification to produce VLR TiO₂ such as chemical additives (electron donors and suppression of backward reaction), noble metal loading, ion doping, sensitization and metal ion-implantation. In this paper, we have made an attempt to review detailed effects of each ion and its different modification techniques to harvest visible light response TiO₂.

2 Background

2.1 History of TiO₂

Ever since the element titanium was discovered, TiO₂ nanoparticles have drawn increasing interests as shown in Table 1 [16-19]. Titanium element was first discovered by William Gregor in 1791, which he called menachanite but was named titanium four years later by Klaproth and the fundamental chemical reactions on which the present titanium industry is based were known before 1800, although it was not available in the markets until 1916 [16]. Titanium dioxide (TiO₂) was discovered in 1821 but it was not until 1916 that modern technology had progressed to the point where it could be massively produced. Fujishima and Honda [20] invented photo-electrochemical splitting of water over TiO₂ to form H₂ and O₂ which opened up greater possibilities of solar energy conversion by semiconductors. The extensive knowledge that was gained during the development of semiconductor photo electrochemistry during the 1970 and 1980's has greatly assisted the development of photocatalysis and its application in the environmental purification. In 1995 TiO₂ was used as a coating on ceramic surface by TOTO Company in Japan [21] while its application for inactivation of pathogenic micro-organisms in air and water was found in 1996. Since then, a number of photocatalyst applications have significantly developed.

Table 1 History and breakthrough of TiO₂

| Year | Comment |
|--------|---------------------------------------------------------------------------------------------------------------------------------------------------------------------------|
| 1791 | - Discovery of the titanium element by Willam Gregor in England |
| 1800's | - Fundamental chemical reactions of titanium |
| 1821 | - Discovery of TiO ₂ |
| 1916 | - Commercial preparation of white pigment TiO ₂ by the sulfate method in Norway |
| 1972 | - Honda-Fujishima effect (photocatalytic reaction) – photo oxidation was used to chemically split water over TiO ₂ to form H ₂ and O ₂ . |
| 1980 | - Photocatalysis on TiO ₂ and Pt/TiO ₂ powder (short circuit photoelectron chemical cell) |
| 1985 | - Photocatalysis on highly dispersed TiO ₂ anchored on various supports - Photocatalysis in the zeolite (cavities and frameworks) |
| 1987 | - Ti/Si and Ti/Al binary oxide photocatalysts - Size quantization effect on the photocatalysis of TiO ₂ - Nanoscale TiO ₂ particles |
| 1990 | - TiO ₂ coating on ceramic surface |
| 1991 | - Idea of sensitized photocatalysis (Grätzel solar cell) |

| | |
|------|-----------------------------------------------------------------------------------------------------------------------------------------|
| | - Purification and detoxification of polluted water |
| 1993 | - Applications of TiO ₂ photocatalysis in the purification of polluted water and air |
| 1996 | - Inactivation of pathogenic microorganism in air and water |
| 1997 | - New function of TiO ₂ thin film photocatalyst (superhydrophilic phenomena) |
| 1998 | - Second generation TiO ₂ in powder and thin film forms (ion-implantation and RF magnetron sputtering method) |
| 2000 | - Applications of TiO ₂ photocatalysts on a global scale |
| 2001 | - Photocatalytic water splitting under visible light irradiation |
| 2006 | - Preparation of TiO ₂ from wastewater sludge for massive, environmental-friendly and functional TiO ₂ production |

2.2 Properties of TiO₂

Titanium is widely distributed over the surface of the earth and is the ninth most abundant element in the earth's crust comprising an estimated 0.62% of the earth crust [22]. The naturally occurring titanium ores are ilmenite, mineral rutile and brookite. Ilmenite is a black sand or rock and has the formula FeTiO₃. The iron is partially oxidized to the trivalent state and ore also contains some impurities of silicon compounds. The TiO₂ concentration in the ore varies from 45% to 60% depending upon the origin. Rutile is naturally occurring TiO₂ and its colour vary from brown to reddish black, and its major impurities are iron compounds. The TiO₂ content in this ore normally varies from 90 to 95%.

Table 2 shows some of the physical and structural properties of TiO₂ [23]. TiO₂ exists in three different phases: anatase, rutile and brookite. TiO₂ is chemically inert and thermally stable, non flammable and non toxic.

Table 2 Physical and structural properties of anatase and rutile structure of TiO₂

| Property | Anatase | Rutile |
|------------------------------|------------------------|------------------------|
| Molecular weight (g/mol) | 79.88 | 79.88 |
| Melting point (°C) | 1825 | 1825 |
| Boiling point (°C) | 2500-3000 | 2500-3000 |
| Specific gravity | 3.9 | 4.0 |
| Light absorption (nm) | $\lambda \leq 385$ nm | $\lambda \leq 415$ nm |
| Mohr's Hardness | 5.5 | 6.5 to 7 |
| Refractive index | 2.55 | 2.75 |
| Dielectric constant | 31 | 114 |
| Crystal structure | Tetragonal | Tetragonal |
| Lattice Constants(A°) | a= 3.784 c= 9.515 | a= 4.5936 c= 2.9587 |
| Density (g/cm ³) | 3.79 | 4.13 |
| Ti-O bond length (A°) | 1.937 (4) 1.965 (2) | 1.949 (4) 1.980 (2) |

Electronic properties such as band gap play an important role for a semiconductor photocatalyst. Anatase phase TiO₂ has higher band gap (3.2 eV) compared with other two phases of rutile (3.0 eV) and brookite. Anatase TiO₂ is more popular as photocatalyst although rutile has been found to be effective under certain specific circumstances [7].

Figure 1 shows the photocatalytic mechanism of water-splitting to produce hydrogen and oxygen and the formation of the precursor species of hydroxyl radical and superoxide ions when illuminated under UV light. The energy level between Valence Band (VB) and Conduction Band (CB) is called band gap. At normal state, electrons and the protons remain in the VB but when TiO₂ is excited by photon with energy greater than its band gap energy level, electrons in the VB jump to the CB, creating e⁻/h⁺ pair. Because of its high band gap of 3.2 eV (anatase), only UV light source has been found to be effective in the excitation of the electrons in TiO₂.

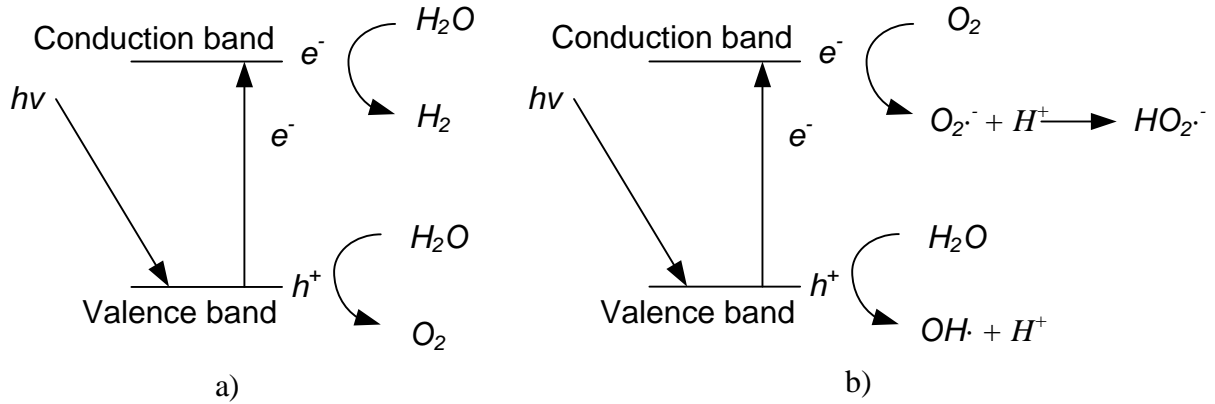
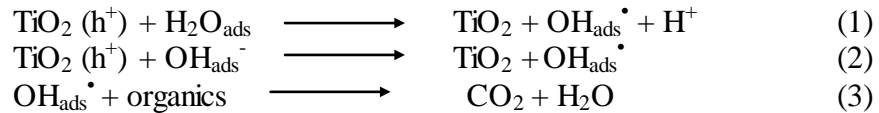


Figure 1 Mechanism of a) photocatalytic water-splitting from hydrogen production and b) formation of reacting species (hydroxyl radicals and superoxide ions) when illuminated under UV light

To produce hydrogen, water should be efficiently broken into hydrogen and oxygen by hydrolysis. When TiO₂ is irradiated by UV light, e⁻/h⁺ pair is formed and when it comes into contact with absorbed water, it gets oxidized by positive holes which in the process forms hydroxyl radicals (OH[•]), having strong oxidative decomposing power and therefore reacts with organic matter. In the presence of oxygen, the intermediate radicals in the organic compounds and oxygen molecules undergo radical chain reactions and consume oxygen to finally form carbon dioxide and water as shown below:



Under certain conditions, organic compounds directly react with the positive holes (h⁺) resulting in oxidative decomposition. In the presence of air, oxygen reduction takes place instead of hydrogen generation and forms superoxide anions (O₂^{•-}) which attach to the intermediate products in the oxidative reaction, forming peroxide or changing to hydrogen peroxide and then later to water.



2.3 Preparation of TiO₂

TiO₂ is produced using a variety of methods such as: i) sulfate method, ii) chloride method (vapor method), iii) alkoxide method, iv) specific method and v) sludge recycling method by Ti-salt flocculation in wastewater [18,19]. Among the methods, the sulphate process and the chlorine process are mainly used to produce TiO₂ powders. World production of TiO₂ is shared almost equally between these two production routes [24]. The chlorine process will continue to displace the sulphate process in the future due to the economic, environmental and market forces. Environmental problems with waste disposal costs associated with the large amount of acid and iron salt wastes which are produced during the sulphate and chlorine process have resulted in the closure of certain U.S based plants [25]. To resolve the above problems, Shon et al. [19] developed a new solution to the sludge problem through a process which recovered economically valuable TiO₂ from wastewater. The work uses titanium tetrachloride (TiCl₄) as an alternative coagulant instead of more commonly used salts of iron (FeCl₃) and aluminum (Al₂(SO₄)₃) to remove particulate and dissolved organic matter including persistent organic pollutant which is not removed in the conventional sewage treatment plants. TiCl₄ coagulant successfully removed organic matter to the same extent as Fe and Al salts and moreover the floc size formed using titanium salt was bigger than that of Fe and Al salts which led to faster and effective settling. This technique is a novel method in solving the environmental problems associated with large quantity of sludge disposal using conventional coagulant. The settled floc was incinerated to produce functional TiO₂ doped with carbon (C) and phosphorus (P) (TiO_{1.42}C_{0.44}P_{0.14}) – and up to 40 mg-TiO₂ per litre of synthetic wastewater was produced following TiCl₄ flocculation.

Alkoxide can be used for the production of high purity TiO₂ and thin film TiO₂. Compared with different TiO₂ preparation methods, TiO₂ by the alkoxide method is free from counter anions so that the effect of the anions on photocatalytic activity is marginal [18]. The alkoxide method is mainly used for TiO₂ coating. When the TiO₂ sol is coated onto a substrate, thin films are obtained which are used for many applications. Specific methods to produce thin film TiO₂ consist of i) thermal decomposition of titanium isopropoxide vapour (amorphous TiO₂ of large surface area), ii) molten salt reaction of a mixture of titanium oxysulfate and alkaline nitrate (microcrystalline anatase TiO₂), iii) laser induced decomposition of alkoxide (TiO₂ microcrystal), iv) hydrothermal oxidation of titanium metal in an autoclave (rutile TiO₂), v) thermal reaction of titanium oxyacetylacetonate in organic media (microcrystalline anatase), v) high temperature hydrolysis of alkoxide with water dissolved in organic solvent (nanocrystalline anatase and higher photoactivity), vi) ultrasonic technique, vii) microemulsion or reverse micelles and viii) thermal decomposition of alkoxide in inert organic solvents and high temperature hydrolysis of alkoxide with water liberated from solvent alcohols (nanocrystalline anatase and higher photoactivity) [26].

2.4 Applications of TiO₂

TiO₂ is the most widely used metal oxide for environmental applications, cosmetics, paints, electronic paper and solar cells. As a pigment, TiO₂ has a remarkably high refractive index and an exceedingly high reflectance. It offers maximum opacity or hiding power as well as imparting whiteness and brightness. The above properties allow TiO₂ as a pigment in paints and coatings (including glazes and enamels), plastics, paper, inks, fibers, food and cosmetics. The material is used as an opacifier in glass and porcelain enamels, sunscreens and cement. As photocatalyst, TiO₂ is used as photosensitizer for photovoltaic cells, and electrode coating in photoelectrolysis cells can enhance the efficiency of electrolytic splitting of water into hydrogen and oxygen. Photocatalytic activity of TiO₂ results in thin coatings of the material exhibiting self cleaning and disinfecting properties under exposure to UV radiation. These properties make the material a candidate for applications such as medical devices, food preparation surfaces, air conditioning filters, and sanitary ware surfaces. As oxygen sensor, even in mildly reducing atmospheres TiO₂ tends to lose oxygen and become sub stoichiometric. In this form the material becomes a semiconductor and the electrical resistivity of the material can be correlated to the oxygen content of the atmosphere to which it is exposed. Hence TiO₂ can be used to sense the amount of oxygen (or reducing species) present in an atmosphere. The followings are the main different applications of TiO₂.

2.4.1 Energy applications of TiO₂

Hydrogen is considered as an ideal fuel for the future. However renewable energy contributes only about 5% of the commercial hydrogen production via water electrolysis, while other 95% hydrogen is mainly from fossil fuels. Nano-sized TiO₂ photocatalytic water-splitting technology has great potential for low-cost, stable, non corrosive, environmentally friendly solar-hydrogen production to support the future hydrogen economy. The solar-to-hydrogen energy conversion efficiency is too low for the technology to be economically sound. The main barriers are the rapid recombination of photo-generated electron/hole pairs as well as backward reaction and the poor activation of TiO₂ by visible light.

In response to these deficiencies, many investigators have been conducting research with an emphasis on effective remediation methods. Some investigators studied the effects of addition of sacrificial reagents to prohibit rapid recombination of electron/hole pairs and backward reactions. The organic compounds act as sacrificial electron donors by consuming photo generated holes and/or oxygen, decreasing the rates of electron-hole recombination and increasing H₂- production rates. EDTA, methanol, ethanol, CN⁻, lactic acid and formaldehyde have been tested and proved to be effective to enhance hydrogen production [27-30]. Moreover, the decomposition of these hydrocarbons could be also contributed to a higher hydrogen yield since hydrogen is one of their decomposed products. Li et al. [27] reported that the addition of cyanide has improved the amount of hydrogen evolution over NiO/TiO₂ which is directly proportional to the cyanide concentration.

When complete liberalization of the sacrificial agent is achieved, the H₂-production rate drops to steady-state values [31]. Photocatalytic decomposition of gaseous methanol on Pt/TiO₂ nano-film can be carried out in a continuous-flow reactor for hydrogen production [32]. The pollutants can be acted as electron donors, so the photocatalytic production of hydrogen and decomposition of these pollutants happened at the same time. The present of carbonate salts was very efficient for hydrogen production using Pt loaded TiO₂ semiconductor photo catalysts [33]. According to Sayama et al. [34] these carbonates salts can prevent backward reaction and thereby enhance the hydrogen production rate. According to Hashimoto et al. [35] the rate of hydrogen production from mixture of water and several aliphatic hydrocarbons when alkaline is added to the solution becomes 2-4 times larger than those without alkaline. Several aromatic compounds also serve as electron donors for the reaction of the present photocatalytic hydrogen production with Pt/TiO₂. The rate of hydrogen production is about 5-10 times larger than those without alkaline. Other researchers focused on the enhancement of photo catalysis by modification of TiO₂ by means of metal loading, metal ion doping, dye sensitization, composite semiconductor, anion doping and metal ion-implantation.

TiO₂ semiconductor photocatalyst loaded with noble metals like Pt can inhibit charge recombination and increase hydrogen production rate [36]. Since Pt is very expensive, low cost metals have been identified. Wu and Lee [28] deposited Cu particles on TiO₂ for hydrogen production from aqueous methanol solution. They reported that the maximum hydrogen production rate was ten times higher than that of blank TiO₂ and 4.5 times higher than P-25 TiO₂ for 1.2 wt% Cu. Anion doping, such as nitrogen doping and sulfur doping, is more effective the photocatalytic activity than metal ion doping [37,38]. Dye sensitization and composite semiconductor are very efficient methods to expand light response of TiO₂ to visible region. Metal ion implantation with wavelength up to 600 nm is a promising modification technique for red shift of TiO₂ photocatalyst. TiO₂ is bombarded with high energy ions which are injected into the lattice and interact with TiO₂. The qualitative effectiveness of red shift observed to be the following order: Cr>Mn>Fe>Ni [39, 40].

The hydrogen evolution rate still remains very low as can be seen from Table 3 [27, 28, 41-43], the apparent energy conversion efficiency defined as the ratio of the combustion heat energy of hydrogen to the radiation energy from the Xe lamp to the reactor. Kida et al. [30] pointed out that according to some estimates an efficiency of 10-15 % might be economical for hydrogen production from water using solar energy.

Table 3 approximately amount of hydrogen evolved after different times for different photocatalysts

| Photocatalyst | Time(hrs) | Amount of hydrogen evolved(micromoles) |
|---------------------------------------------------------------------|-----------|----------------------------------------|
| Aqueous 1 mmol KCN and 1.5M NaOH with NiO/TiO ₂ catalyst | 1 | 370 |
| | 2 | 480 |
| | 4 | 1000 |
| Deposition TiO ₂ with Cu particles from aqueous | 1 | 3000 |

| | | |
|-----------------------------------------------------------------------------------|---|------|
| methanol solution | 2 | 4200 |
| | 4 | 6200 |
| 100ml of 4.9×10^{-3} M oxalic acid solution; 0.05 g | 1 | 60 |
| 0.5 wt.% Pt-TiO ₂ | 2 | 115 |
| | 4 | 220 |
| Ar-calcined TiO ₂ from water-methanol solution | 1 | 1200 |
| (vol.ratio =1.4/1) | 2 | 1400 |
| | 4 | 1450 |
| N-doped TiO ₂ (0.1g) in 0.2 M Na ₂ SO ₃ solution | 1 | 270 |
| from Urea and titanium tetrachloride (mole ratio | 2 | 450 |
| Urea/TiO ₂ = 5) | 4 | 1080 |

Based on the studies reported in the literature, metal ion-implantation and dye sensitization are very effective methods to extend the activating spectrum to the visible range [15]. They play an important role in the development of efficient photocatalytic hydrogen production to more than 10-15% under sunlight.

2.4.2 TiO₂ applications to air purification

The applications of photocatalysis have been expanded, and it has become more attractive. An air treatment system for ethylene removal has been placed in grocery stores to remove the naturally occurring ethylene that causes fruits and vegetables to spoil. TiO₂ photocatalytic reactor traps and chemically oxidizes volatile organic compounds converting them primarily to carbon dioxide and water. Photocatalytic reactors are also modular and can be scaled to suit a wide variety of air quality applications. They operate at room temperature and with negligible pressure drop and therefore may be readily integrated into new and existing heating, ventilation, and air conditioning systems [44]. TiO₂ catalyst which is excited by plasma-induced high-energy particles (electrons, photons), resulting in an enhanced pollutant air removal cleaning system for such as tobacco smoke found in indoor environments [45]. Thin films of organic contaminants can be photocatalytically oxidized on TiO₂-coated surfaces. The thickness of the organic layer oxidized per day is 1-5 pm, a rate sufficient for maintaining the cleanliness of a surface when the flux of contaminant is not excessive [46]. In the process of treating air streams, TiO₂ must be suspended on some sort of surface to allow the gas to pass over it and react. This is usually some sort of matrix with a high surface area and UV light.

The main purpose of photocatalytic coatings is to maintain clean windows or windshields, strip finger marks off walls and to reduce the density of colonies of microorganisms on hospital walls. Toluene and formaldehyde are malodorous and cause indoor pollution. Ichiura et al. [47] prepared a composite sheet of TiO₂-zeolite using a papermaking technique to decompose formaldehyde and toluene under UV irradiation. It was shown that these sheets are potentially applicable as highly functional materials to be placed on walls and ceilings of houses.

TiO₂ can be used to coat building materials, such as glass, tile, and cement [48]. Once coated, these sidings, roofs, or roads could remove outdoor air pollutants. These

pollutants are converted into carbon dioxide and water vapor. Coating roadway systems are being considered for air pollution mitigation [49], and has already been used on several building structures in Italy [50, 51]. Most of the exterior walls of buildings become soiled from automotive exhaust fumes, which contain oily components. When the original building materials are coated with a photocatalyst, a protective film of titanium provides the self-cleaning building by becoming antistatic, super oxidative, and hydrophilic. The hydrocarbon from automotive exhaust is oxidized and the dirt on the walls washes away with rainfall, keeping the building exterior clean at all times [52].

The glass covers on highway tunnel lighting fixtures darken from automobile exhaust, when TiO_2 coated lamp covers are used, the glass surface remains cleaner longer, and the number of required cleanings is greatly reduced [21]. The Japanese company TOTO developed TiO_2 -coated surfaces tiles for operating rooms, hospital applications and public restrooms on the basis of joint research with Fujishima, Hashimoto and their colleagues at the University of Tokyo [46]. Colonies of pathogenic microorganisms do not persist on them, even under low level irradiance from common fluorescent lamps.

TiO_2 coatings on sintered borosilicate glass were prepared employing a synthetic route based on the hydrolysis of titanium oxysulfate (TiOSO_4) [53]. The stability and lifetime of the coatings were tested for more than 4000 hrs of continuous operation. They have not noticed any appreciable degradation of the coatings was observed.

Air purifier with TiO_2 can prevent smoke, soil, pollen, bacteria, virus and harmful gas as well as seize the free bacteria in the air by filtering percentage of 99.9% with the help of the highly oxidizing effect of photocatalyst TiO_2 [54]. It was powerful for the sterilization of floating germs. They noticed that the number of germs after seven months operation were almost the same as obtained in the first operation. Ao and Lee [55] have used TiO_2 immobilized on activated carbon (TiO_2/AC) filter for removing indoor air pollutant which was installed in an air cleaner. They found that the higher removal efficiency of using TiO_2/AC filter is owing to the large adsorption capacity provided by the activated carbon. A 25% higher of nitrogen oxides (NO_x) was achieved using TiO_2/AC filter compared to the TiO_2/AC only. Purification ability of TiO_2/AC was found to be higher than single purification techniques in decomposing toluene, whether in high concentration or low concentration [56]. They found that the compound of TiO_2 photocatalyst and active carbon has the advantage of active carbon absorption and TiO_2 photocatalyst for decomposition.

2.4.3 Water applications of TiO_2

Photocatalyst coupled with UV lights can oxidize organic pollutants into nontoxic materials, such as CO_2 and water and can disinfect certain bacteria in water. This technology is very effective in removing further hazardous organic compounds and at killing a variety of bacteria and some viruses in the secondary wastewater treatment. Heterogeneous photocatalysis is an alternative treatment method for decontamination of organic compounds and disinfection of microorganisms to purify potable water [57].

Disinfecting microorganisms such as E.coli is a great concern in drinking water supply facilities around the world. An annular type fluidized bed reactor has been constructed and tested to disinfect E.coli bacteria [58]. They prepared specially catalyst of (TiO₂ + glass bead + zeolite). The efficiency of E.coli removal was 99.99% by using the proposed technology. It has been found that the pilot scale is capable of degrading 84% of E.coli within 80 minutes compared with 77.3% by using UV only which has capacity of handling 46 litre/min. E.coli degradation in larger scale is being tested for the first time and its result compared with only UV destruction is promising. They recommended using this method on a continuous reactor to increase the potential for scale up. Peyton and DeBerry [59] used three different semiconductors (TiO₂, ZnO, and Fe₂O₃) to decompose pollutant compounds in wastewater by using solar energy. They concluded that Fe₂O₃ was found to be ineffective, both ZnO and TiO₂ catalyzed the removal of all compounds.

Yamashita et al. [60] has used the metal ion-implantation method to improve the electronic properties of the TiO₂ photocatalyst to realize the utilization of visible light. They investigated the properties of TiO₂ photocatalyst for the purification of water. The UV-VIS absorption spectra of these metal ion-implanted TiO₂ photocatalysts were found to shift toward visible light regions depending on the amount and the kind of metal ions implanted. They were found to exhibit an effective photocatalytic reactivity for the liquid-phase degradation of 2-propanol diluted in water at 295 K under visible light ($\lambda > 450$ nm) irradiation. Zhanghai et al. [61] fabricated a composite nano-ZnO/TiO₂ photocatalyst with vacuum vaporized and sol-gel methods. They indicated that the nano-ZnO/TiO₂ film improved the separate efficiency of the charge and extended the range of spectrum, which showed a higher efficiency of photocatalytic than the pure nano-TiO₂ and nano-ZnO film. Under the optimal operation conditions, chemical oxygen demand (COD) values with the linear range of 0.3–10.0 mg Γ^{-1} were achieved and these results were in good agreement with those from the conventional COD methods. Photocatalysis aided by TiO₂ nanoparticles is used in removing the organic chemicals which occur as pollutants in wastewater effluents from industrial and domestic sources.

In general, the main advantage of photocatalysis is that there is no further requirement for secondary disposal methods. Other treatment methods such as adsorption by activated carbon and air stripping merely concentrate the chemicals present by transferring them to the adsorbent or air and they do not convert them to non toxic wastes. Also as compared to other oxidation technologies, expensive oxidation methods are not required as ambient oxygen is used.

2.4.4 Pigment applications of TiO₂

The most important function of TiO₂ however is in powder form as a pigment for providing whiteness and opacity to such products such as paints and coatings (including glazes and enamels), plastics, paper, inks, fibers and food and cosmetics. TiO₂ is by far the most widely used white pigment. TiO₂ very white and has a very high refractive index – surpassed only by diamond. The refractive index determines the opacity that the material confers to the matrix in which the pigment is housed. Hence, with its high

refractive index, relatively low levels of TiO_2 pigment are required to achieve a white opaque coating.

The high refractive index and bright white colour of TiO_2 make it an effective opacifier for pigments. The material is used as an opacifier in glass and porcelain enamels, cosmetics, sunscreens, paper, and paints. One of the major advantages of the material for exposed applications is its resistance to discoloration under UV light. Even in mildly reducing atmospheres TiO_2 tends to lose oxygen and become sub stoichiometric. In this form the material becomes a semiconductor and the electrical resistivity of the material can be correlated to the oxygen content of the atmosphere to which it is exposed. Hence TiO_2 can be used to sense the amount of oxygen (or reducing species) present in an atmosphere.

2.4.5 Applications of TiO_2 in construction materials

TiO_2 photocatalyst have high application potential in the construction industry. Many applications of this material already exist, such as photocatalytic ceramics, self cleaning glass, photocatalytic cements and paints. TiO_2 coating makes the material surface super hydrophilic and self-cleaning. Thin coating not only makes the surface wetting and rinsing more uniform so that water slides easily without forming a droplets and float away organic surface contaminants. Moreover the organic dust that may come in contact with the surface will be removed by photocatalytic action in presence of sun light. This technology has allowed the creation of many exterior and interior facades and self-cleansing rooftops from ceramic and glass tiles [62]. More applications could be found in the future for building applications such as self cleansing pavements, walls, tunnels, curbs so on to remove NO_x and SO_x from the air produced by vehicular emissions.

Photocatalyst-modified cements are used for various applications in buildings, self-cleaning surfaces and solar-powered dremediation devices for polluted waters [63]. They used a model reaction of photocatalytic atrazine degradation by white Portland cement samples modified with different semiconducting oxides TiO_2 to investigate a possible application of modified cements for the degradation of pollutants on building surfaces.

2.4.6 Applications of TiO_2 in waste treatment

The most common water treatment technologies for hazardous organic pollutants is using adsorption on granulated activated carbon and air stripping to destroy the contaminants. Its implementation on a large scale was prevented due to negative public perception and the potential hazard of incineration of organic toxic compounds. Hofstadler and Bauer [64] recommended that one of the most effective approaches to resolve this problem is the mineralization of organic contaminants by using photocatalytic semiconductors (SrTiO_2). They indicated that the potential is high enough to destroy most organic compounds to carbon dioxide and mineral acids.

Photocatalytic degradation using ultraviolet-irradiated TiO_2 suspension has been investigated for destroying both free and complex cyanide with a concurrent removal of

copper metal [65]. In contrast to conventional cyanide waste treatment processes, the photocatalytic processes convert both free and complex cyanide species into carbon dioxide and nitrogen with no residual harmful chemicals remaining. Results revealed that about 78% of free cyanide (10^{-3} M) was removed after illumination for 4 hours in the presence of 1 g/L TiO_2 at pH 11. Free copper (10^{-2} M) was completely removed in a shorter time of 3 hours.

2.4.7 Oil spills applications for TiO_2

Oil spills in the sea and ocean is one of the major environmental disasters in the marine environment. Researchers have been trying to study the effect of photodegradation in cleaning up the marine environment. The application of TiO_2 photocatalysis has therefore been reported for the remediation of marine environment [66-68].

Photodegradation remains one of the least studied related to the crude oil and petroleum products spilled into the ocean or coastal waters. In fact, all the weathering process occurred simultaneously in the environment, and it is difficult to distinguish the changes induced by photodegradation from the changes induced by other process as biodegradation. Furthermore, the complex composition of crude petroleum and oil fractions makes the photodegradation process complicated. A multitude of photoinduced reactions could take place, producing also a multitude of photodegradation products. Polycyclic aromatic hydrocarbons (PAHs) frequently appear in oil spills, petroleum fractions and coal. The possible applications in the cleaning up of marine oil spills have been considered [69]. The initial photoreactivity of petroleum distillates was found to depend greatly upon the aromatic fraction. PAHs are a class of persistent organic pollutants of special concern since they are carcinogenic and mutagenic [70]. PAHs were identified as the photosensitizing species responsible for most of the initiation reactions. An aromatic rich distillate photodegrades about ten times faster than a homologue distillate with low aromatic content [71].

The PAHs reached a high degree of photodegradation in the water-soluble fraction, but the heavier PAHs have fewer tendencies to photodegradation. However, the organic fractions remained almost unaffected. The alkyl derivatives of PAHs show lower photodegradation rates than parent compounds (those without radical substituents). In general, the photodegradation rate lowers with the increasing substitution [68].

Photodegradation is in some cases as important as biodegradation, since these two processes act upon different components of oil: alkanes are biodegraded while aromatics tend to be photodegraded, and this fact leads to synergistic reactions which enhance the degradation of oil [72]. However, the *n*-alkanes with 10 or more carbon atoms and the isoprenoids such as pristane and phytane are very resistant to photodegradation [73], while in crude oil the secondary and the tertiary alkanes are easier to photodegrade. *N*-alkanes were easily degraded by marine bacteria, while branched and cyclic alkanes were assumed to be less biodegradable [74]. Photoinduced toxicity of oil and PAHs has been confirmed due to the transient photodegradation intermediates which showed higher

toxicity and solubility than the initial compounds, but were subsequently destroyed in the photocatalytic process [75].

Photocatalytic oxidations of dodecane and toluene have been considered in pure water and in synthetic sea water on different TiO₂ powders under simulated solar radiation. Minero et al. [67] indicated that diluted hydrocarbons disappear in pure water in the presence of TiO₂ and simulated solar radiation. The current properties of pure TiO₂ have been found to be effective only under UV irradiation and hence there are still more challenges for in-situ application of TiO₂ in open sea or water bodies.

2.4.8 Disinfections applications of TiO₂

Photocatalyst does not only kill bacteria cells, but also decompose the cell itself. The TiO₂ photocatalyst has been found to be more effective than any other antibacterial agent, because the photocatalytic reaction works even when there are cells covering the surface and while the bacteria are actively propagating [76]. The end toxin produced at the death of cell is also expected to be decomposed by photocatalytic action. TiO₂ does not deteriorate and it shows a long-term anti-bacterial effect. Generally speaking, disinfection by TiO₂ is three times stronger than chlorine, and 1.5 times stronger than ozone. Bacteria and viruses are decomposed on the tile surface due to the strong oxidizing properties of TiO₂. If you cover the walls, ceiling and floor with photocatalytic tiles, bacteria floating in the air in an operating room are also killed as they come in contact with the TiO₂ surface [21].

2.4.9 Soil application of TiO₂

One of the other applications of TiO₂ photocatalysis is the remediation of organically contaminated soil and sludge. Both pure and composite photocatalyst has been tried for the removal of organic pollutants from soil. Xie et al. [77] investigated the enhancement of photo degradation of organics on soil surfaces using TiO₂ induced by UV-light. They concluded that the photodegradation rate increased with the increase of the soil pH and photon flux. Higrashi and Jardim [78] used heterogeneous photocatalytic of TiO₂ to degrade pesticide (diuron) under laboratory conditions to evaluate the potential use of this technology for in situ remediation. They reported that the photocatalytic treatment combined with solar light to be very efficient in the destruction of diuron in the top 4 cm of contaminated soil, with the degradation rate markedly dependent on the irradiation intensity.

Pelizzetti et al. [79] mixed contaminated soils of 2-chlorophenol, 2,7-dichlorodibenzodioxin and atrazine with a photocatalyst (TiO₂) in a aqueous slurry and exposed them to simulated solar radiation in the laboratory. They noticed that the organic contaminants were destroyed in relatively short time and reported that the photocatalytic processes could be effective chemical detoxification methods for contaminated soils. According to Hamerski et al. [80] the most active photocatalyst for soil purification was TiO₂ modified by calcium.

The common challenge on the above TiO₂ applications is to use its photoactivity under visible light irradiation. Thus, the following sections focus on the modification of VLR TiO₂.

3.0 Modification of TiO₂ to harvest visible light

Heterogeneous photocatalysis using semiconductor TiO₂, is a fast growing field of basic and applied research for the degradation of organic pollutants in water and in air and photocatalytic water-splitting for hydrogen production [78, 81-83]. Oxidation of organic pollutants occurs because of the electron-hole pairs of the semiconductor after being excited by UV light with energy equal to or greater than the band gap energy (E_g) of semiconductor. TiO₂ is considered the noble photocatalyst because of its many intrinsic properties, but it has its own limitations which are critical to photocatalytic technology [84] such as: i) recombination of photo-generated electron/hole pairs, ii) fast backward reaction and iii) inefficient visible light utilization. The other significant drawback of TiO₂ as photocatalyst is its wide band gap because it is found effective only under UV irradiation and not under solar light that contain only about 4% of UV rays [5,7]. The use of UV as light source has many disadvantages such as requirement of external energy and also has to be conducted in a closed and protected space. Therefore in order to deal with these drawbacks, techniques such as i) addition of electron donors (hole scavengers), ii) addition of carbonate salts, iii) noble metal loading, metal ion doping, iv) anion doping, v) dye sensitization, vi) composite semiconductors and vi) metal ion-implantation have extensively been investigated [15].

Several attempts have been made to modify UV responsive TiO₂ to VLR TiO₂ and one of the methods is by doping of TiO₂ with other substances. Sol-gel method is one of the most popular methods used for doping TiO₂. Mechanical alloying is also an effective process for refining grain size down to the nano-sized range and has the ability to alloy immiscible elements. In hydrothermal method the products prepared have well crystalline phase and have high thermal stability of the nano-sized materials. Flame spray pyrolysis is the coupling of high temperature and rapid quenching has been found to generate homogeneous doping even at a concentration level as high as 30 wt.%. Ion-implantation technique is used for doping at higher concentrations of dopants up to 60% and it gives better properties of powders than sol-gel method.

Doping of TiO₂ using noble metals such as gold [85,86], silver [6, 87, 88], platinum [5,89] transition metal ions such as Co, Cr, Cu, Fe, Mo, V and W [1,90,91], non-metals such as C, N, P and S [7,37 , 83, 92], carbon, coupling with organic dye-sensitizers [93-95] have been reported and also shown a promising result under visible light irradiation though the mechanism under which this process occurs still remains controversial. The followings are some of the attempts made to modify the electronic structures of TiO₂ to improve its effectiveness under visible light.

3.1 Noble metal loading (Pt, Au, Pd, Rh, Ni, Cu, Sn, Ag)

Noble metals deposited or doped on TiO₂ (Pt, Au, Pd, Rh, Ni, Cu, Sn and Ag) show various effects on the photocatalytic activity of TiO₂ by different mechanisms [88]. These noble metals act separately or simultaneously depending on the photoreaction conditions and they may (i) enhance the electron–hole separation by acting as electron traps, (ii) extend the light absorption into the visible range and enhance surface electron excitation by plasmon resonances excited by visible light and (iii) modify the surface properties of photocatalyst. While some authors have reported an increased photocatalytic activity under visible light due to certain metal ion doping, others have reported a decreased activity. But generally the photocatalytic property of metal ion doped TiO₂ has been reported to be quite higher than the undoped TiO₂ and therefore is seen to be of very high research value.

The effect of platinum (Pt) loading on TiO₂ was mainly studied for hydrogen generation from water but it was also observed that it increases the degradation of organic pollutants. Pt ion doped TiO₂ has been reported to have not only high photocatalytic activity under UV irradiation but also effective under visible light irradiation. Kim et al. [5] successfully demonstrated the visible light photocatalytic degradation of chlorinated organic compounds using Pt doped TiO₂. It had lower band gap than that of undoped TiO₂ by about 0.2 eV and it showed higher photocatalytic activity than undoped TiO₂. Analyses showed that Pt ions were substituted in the TiO₂ lattice and the visible light absorption is due to electronic transition between the band gap edge (CB or VB). The defect redox states of Pt ions substituted in the TiO₂ lattice. It was also found that the visible light activity of Pt-TiO₂ was observed to be strongly affected by the calcination temperature. Nano-Ag doped TiO₂ was investigated [88] and observed that the Ag clusters give rise to localized energy levels in the band gap of TiO₂ and the VB electrons of TiO₂ are excited at wavelength longer than 370 nm. The photonic efficiency increases with an increase in the metal loading up to an optimum level while above the optimum level, the dopants behave as electron/hole recombination centres. Under UV irradiation, Ag deposits exhibit the effect only as electron traps, thus leading to the enhancement in the Ag-TiO₂ photocatalytic activity. The substitution of Sn for Ti in the lattice structure is expected to aid the formation of solid solutions, alter the structure and contribute to the thermal stability of TiO₂ [96]. More details of the noble metal loading are shown in Table 4.

Table 4 Characteristics of noble metal loading on TiO₂

| Noble metal | Remarks |
|-------------|-------------------------------------------------------------------------------------------------------------------------------------------------------------------------------------------------------------------------------------------------------------------------------------------------------------------------------------------------------------------------------------------------------------------------------------------------------------------------------------------------------------------------------------------------------------------------|
| Pt | - Pt loading reduced the amount of Ti ³⁺ (evidence of the occurrence of electron transfer from TiO ₂ to Pt) [97]. - Pt showed better than Au loading in terms of hydrogen generation [36]. |
| Ag | - Anatase size (at 600°C) decreased from 37 nm to 19 nm. Specific surface area increased from 45 m ² /g to 63 m ² /g. Photocatalytic activity increased by 18%. Phase transfer appeared from anatase to rutile at 700°C and phase transformation was completed at 800°C [98]. - Ag/TiO ₂ catalyst was evaluated for the photocatalytic degradation of reactive yellow-17 under UV and visible light irradiations. The enhanced degradation of reactive yellow-17 was obtained with Ag-deposited TiO ₂ due to trapping of |

| | |
|----|--------------------------------------------------------------------------------------------------------------------------------------------------------------------------------------------------------------------------------------------------------------------------------------------------------------------------------------------------------------------------------------------------------------------------------------------------------------------------------------------------------------------------------------------------------------------------------------------------------------------------------------|
| | conduction band electrons [99]. |
| Au | - Optical characterization by UV–vis spectrophotometer showed a shift in optical absorption wavelength to visible region which may be due to the incorporation of gold nanoparticles (1-2%) into TiO ₂ structure. The kinetic study showed that the rate of decomposition of phenol using Au/TiO ₂ photocatalyst was improved by 2 – 2.3 times than undoped TiO ₂ [100]. - Au/TiO ₂ (0.45 wt %) in the oxidation of glucose resulted in high selectivity and high catalytic activities were made in the optimum conditions at a reaction temperature (40–60 °C) and a pH value [101]. |
| Pd | - Loadings of Pt and Au were better than that of Pd due to suitable electron affinity [102]. - Pd/TiO ₂ anatase exhibited higher acetylene conversion and ethylene selectivity than rutile TiO ₂ supported ones. Ag addition to Pd/TiO ₂ anatase suppressed the advantageous effect of the Ti ³⁺ sites during selective acetylene hydrogenation [103]. |
| Cu | - Cu loading was almost comparable to Pt loading for hydrogen production. - The optimum contents for Cu (1.5 wt.%), Pd (1 wt.%), and Au (2 wt.%) loadings produced the H ₂ evolution rate of 360, 420, and 557 μmol/h, respectively, suggesting that the H ₂ evolution resulted showed that the photocatalytic capability of the cocatalysts was in the order of Au > Pd > Cu [104]. |
| Ni | - Ni and Ag loadings among different noble metals were found to be effective for photocatalytic activity [105]. |
| Sn | - At 500°C a mixture of anatase and rutile phases was observed with rutile. |

3.2 Ion doping

Cationic and anionic elements have been used as either dopants or simply as deposited with TiO₂ to increase its photocatalytic activity under visible light region. The Ti ions in TiO₂ has been substituted with different metal ions by metal ion implantation or metal doping as shown in Figure 2 for increasing its photocatalytic properties. On the other hand, the substitution of O ions in TiO₂ with N, S, C, F and P ions has also been reported to enhance its visible light response (Figure 2) but the effectiveness of doped TiO₂ as photo anode or as photocatalyst critically depends on the preparation and doping methods [106].

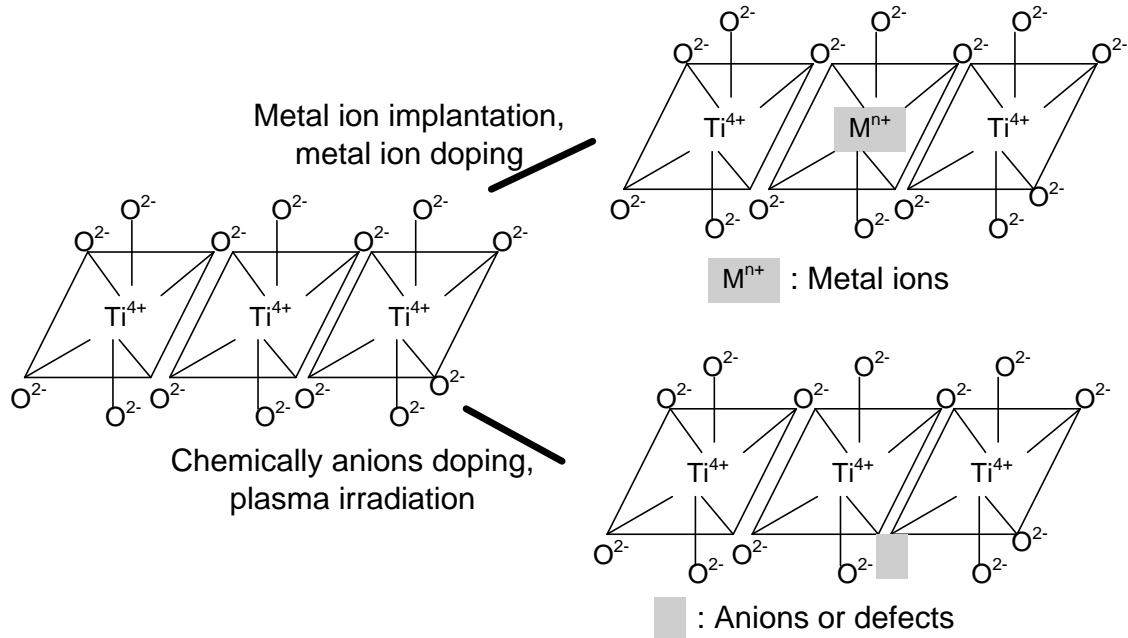


Figure 2 Electronic structure of TiO_2 by the substitution of metal ions or anions to harvest visible light response [10]

3.2.1 Cationic (Metal) Doping (Fe, V, Mo, Ru, Os, Re, V, Rh, Mn, Ni, Co, Cr, La, Ce, Er, Pr, Gd, Nd, Sm, Zn)

The majority of the metal-ion-doped TiO_2 photocatalysts studied were prepared using the coprecipitation, incipient wet impregnation method and sol-gel method [107]. Transitional metal and rare earth metal ions have been tried as dopants to improve the photocatalytic efficiency of TiO_2 in the visible light region. As metal ions are doped into TiO_2 , impurity energy levels in the band gap are formed. This leads to the alteration of electron hole recombination. Transitional metals are either deposited or doped on the TiO_2 surfaces as metallic nanoparticles or the metals are doped as ionic dopants. A common method consists of doping of TiO_2 with transition metal cations while maintaining a good control of the primary particle size to achieve nanoscale configurations of the catalysts. The doping elements usually are Cr, Fe, V, Nb, Sb, Sn, P, Si, and Al [108].

Iron has been used to dope TiO_2 and its photocatalytic activity was superior than the commercial Degussa P-25 under visible light irradiation [91]. Teoh et al. [109] also reported that Fe-doped TiO_2 was found to have very high photocatalytic activity under visible light irradiation than Degussa P-25. Fe^{3+} cations acted as shallow traps in the TiO_2 lattice. Optimum photocatalytic properties were achieved upon doping at a relatively weak level. This was closely related to the dynamics of the recombination process which was linked to the distance between dopant cations in the TiO_2 lattice [110]. Fe ions trapped not only electrons but also holes, which leads to increase of photoactivity [111]. The maximum photoactivity appeared with 0.5 wt% of Fe^{3+} due to decrease in the density of the surface active centers [14]. The added Fe atoms dissolved in TiO_2 phase

was found to have a rutile structure with average grain size less than 10 nm. Fe-doped powder had a higher absorption threshold in the range of 427-496 nm than the commercial P-25 powder (406 nm). Fe-doped powder color changed from white to bright yellow, Fe content more than 4.57 wt% decreased the UV-Vis absorption turning the bright yellow to dark yellow.

Vanadium doped TiO₂ and its visible light activities have been reported [2,112-118]. A vanadium-doped TiO₂ is reported to have shown quite high photocatalytic property under visible light irradiation. It is believed that under visible light irradiation the excited vanadium centres donate electron to the TiO₂ CB, which allows the oxidation of surface adsorbed molecules [2]. Vanadium is thus a rather interesting candidate to obtain valuable TiO₂-doped photocatalysts. The photocatalytic activity of Eu³⁺-, La³⁺-, Nd³⁺- and Pr³⁺-doped TiO₂ was investigated [119] and observed that these doped nanoparticles showed high photocatalytic activity in comparison to undoped TiO₂ and their analysis indicated that this was attributed to the increased charge separation in the doped systems. Various transition-metal cation dopants have been extensively investigated. However the disadvantage of cationic dopants is that they can result in localized d-levels deep in the band gap of TiO₂, which often serve as recombination centers for photo-generated charge carriers [3]. Figure 3 shows effect of different metals in TiO₂ to absorb visible light and to enhance photocatalytic activity [56,120,121]. More details of the cation doping TiO₂ are shown in Table 5.

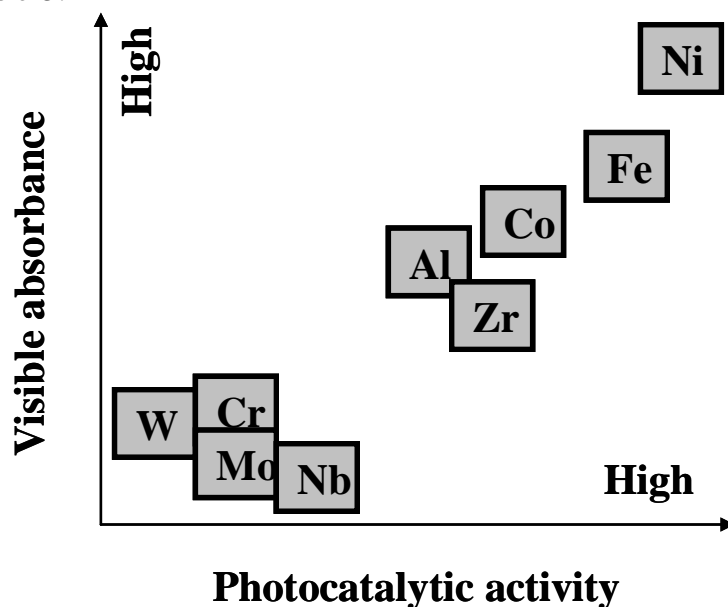


Figure 3 Effect of cationic doping compounds in terms of visible light absorbance and photocatalytic activity

Table 5 Characteristics of cationic doped TiO₂

| Cation | Remark |
|--------|-----------------------------------------------------------------------------------------------------------|
| Fe | - Fe ³⁺ cations acted as shallow traps in the TiO ₂ lattice. Optimum photocatalytic |

| | |
|-------------------|------------------------------------------------------------------------------------------------------------------------------------------------------------------------------------------------------------------------------------------------------------------------------------------------------------------------------------------------------------------------------------------------------------------------------------------------------------------------------------------------------------------------------------------------------------------------------------------------------------------------------------------------------------------------------------------------------------------------------------------------------------------------------------------------------------------------------------------------------------------------------------------------------------------------------------------------------------------------------------------------------------------------------------------------------------------------------------------------------------------------------------------------------------------------------------------|
| | <p>properties were achieved upon doping at a relatively weak level. This was closely related to the dynamics of the recombination process which was linked to the distance between dopant cations in the TiO₂ lattice [110].</p> <ul style="list-style-type: none"> - Fe and Cu ions trapped not only electrons but also holes, which led to increase of photoactivity [111]. - The maximum photoactivity appeared with 0.5% of Fe³⁺ (weight) due to decrease in the density of the surface active centers [14]. - The added Fe atoms dissolved in TiO₂ phase was found to have a rutile structure with average grain size less than 10 nm. Fe-doped powder had a higher absorption threshold in the range of 427-496 nm than the commercial P-25 powder (406 nm). Fe-doped powder color changed from white to bright yellow, Fe content more than 4.57 wt.% decreased the UV-Vis absorption turning the bright yellow to dark yellow. |
| Cr, Fe, V, Nb, Si | <ul style="list-style-type: none"> - Anatase-to-rutile transformation was accelerated by the mmol% content of Nb, Cr, Si, and Fe in TiO₂. Interaction of co-precipitated or impregnated cations was found critical in the phase transformation process. Nb retarded the crystal growth during calcinations [108]. |
| Al | <ul style="list-style-type: none"> - Aluminium doping was used on TiO₂ for a potential application in thermal shock due to its stable thermal expansion coefficient and physical property [122]. Al₂O₃ and Al₂TiO₅ were observed at AlCl₃/TiCl₄ ratios higher than 1.1 at 1400 °C. They found that a new structure connected with Al-O-Ti framework was generated. For Al/TiO₂, the anatase structure was stable after calcination at 800 °C, while pure TiO₂ was easily transferred to the rutile phase after calcination above 700 °C. The optical property of Al/TiO₂ prepared by a thermal plasma method responded visible light [123]. They also found that the size of synthesized powder decreased with increase of the amount of Al because Al species inhibited the particle growth. Al/TiO₂ was applied to gas sensor, which needed high conductivity of TiO₂ [124]. It has been reported that the conductivity of the Al-doped TiO₂ is higher than that of pure TiO₂ in a temperature (600 – 900 °C) |
| V | <ul style="list-style-type: none"> - V doping made in the sol-gel method provided a promising method to enhance the photoactivity of TiO₂ under visible light [125]. |
| Li | <ul style="list-style-type: none"> - TiO₂ doped with Li ions resulted in significant improvement in the rate of phenol degradation. On the other hand, Co, Cr, Mn, Ce, Al and Fe doped TiO₂ (5 mol %) was inactive in removing phenol [14]. - The crystalline size increased from 20 to 27 nm. The photocatalytic activity decreased. |
| Na, K | <ul style="list-style-type: none"> - Na-doped TiO₂ decreased the nanoparticle size from 20 nm to 11 nm. The photocatalytic activity decreased. - K-doped TiO₂ decreased the size from 22.4 to 7 nm. The photocatalytic activity decreased. |
| Cu, Mn | <ul style="list-style-type: none"> - Cu, Mn and Fe ions trapped electrons and holes and these ions worked better than Cr, Co and Ni ions [42]. |
| Co | <ul style="list-style-type: none"> - Among the 21 metal ions doped, Fe, Mo, Ru, Os, Re, V and Rh ions increased photocatalytic activity, whereas Co and Al ions caused detrimental effect [112]. |
| Gd | <ul style="list-style-type: none"> - Gd, La, Ce, Er, Pr and Nd doped with TiO₂ changed to red shift. Among them, Gd ions showed effective photoactivity and transfer of charge carriers [126]. |

3.2.2 Anionic (non-metal) doping (C, N, S, P, F)

Anionic or non-metal dopants, namely, carbon (C), sulphur (S), nitrogen (N), phosphorus (P) and fluorine (F), are being investigated to extend the photocatalytic activity into the

visible light region. It is said that the related impurity states are supposed to be close to the valence band maximum. Furthermore, the position of the conduction band minimum, which must be kept at the level of the H_2/H_2O potential, when TiO_2 is used for the photoelectrolysis of water into hydrogen and oxygen, is not affected [3].

N-doped TiO_2 can be made by i) heating of titanium hydroxide and urea, ii) reactive magnetron sputtering, iii) nitriding of anatase TiO_2 with alkylammonium salts and iv) treating TiO_2 powder in NH_3 (80%)/Ar gas flow at 550 °C [15]. Sato [128] firstly reported the visible light activity of TiO_2 -based products from the calcinations of $Ti(OH)_4$ and ammonium salts and ascribed this beneficial doping effect to NO_x impurities on the TiO_2 lattice. Recently many groups have concluded that the visible light photoactivity was due to oxygen vacancies which gave rise to donor states located below the conduction bands, while the substitutional nitrogen acted as an inhibitor for electron-hole pair recombination. Asahi et al. [37] recently suggested that when N (2p) states and O (2p) states were mixed, the resultant band gap of nitrogen doped TiO_2 was reduced below intrinsic band gap edge and the photoactivity under visible light due to substitutional nitrogen atoms. Irie et al. [128] concluded that nitrogen-induced effect allowing sub-band gap excitation was due to an isolated N (2p) states rather than band gap narrowing. Optical absorption identified the substitutional-doping and localized N-states in the TiO_2 lattice and the status of N to be anion-like (N-) and the chemical environment of N was in N-Ti-O in the TiO_2 lattice [83]. Absorption below 500 nm was mainly due to nitrogen states located above the valence bands, whereas absorption above 500 nm was mainly caused by oxygen vacancies [128]. Valentin et al. [130] observed that nitrogen caused a significant change in the absorption spectra of the TiO_2 and showed that the N 2p orbitals were localized above the top of the O 2p valence bands, even for relatively large values of doping. The N-doping effects on the electronic and optical properties of TiO_2 rutile crystal have been studied using density functional theory [131]. Their calculations of several possible N-doped structures showed that band gaps had little reduction but some N 2p states lay within the band gap in the substitutional N to O structure and interstitial N-doped rutile supercell, which resulted in the reduction of the photon-transition energy and absorption of visible light. In contrast, substitutional N to Ti doped model had a significant band-gap narrowing.

Carbon-doped TiO_2 thin films had hydrophilic property under visible light irradiation [132]. The localized C (2p) formed above the valence band should be the origin of visible light sensitivity, which resulted in an inferior hydrophilic property when irradiating with visible light compared with UV light. Park et al. [85] reported the preparation of vertically grown carbon-doped TiO_2 ($TiO_{2-x}C_x$) nanotube arrays with high aspect ratios for maximizing the photocleavage of water under white-light irradiation. The synthesized $TiO_{2-x}C_x$ nanotube arrays showed much higher photocurrent densities and more efficient water splitting under visible-light illumination (> 420 nm) than pure TiO_2 nanotube arrays. The total photocurrent was 20 times higher than that with a P-25 nanoparticulate film under white-light illumination.

Wushu et al. [133] prepared S-doped nano- TiO_2 catalysts which showed photocatalytic activity under visible light. They observed that S-doped TiO_2 greatly increased grain

distribution, a uniform dispersion of nanocrystals fabrication; In addition, S-doped TiO₂ in the treatment effectively inhibited the process of transformation from anatase to rutile. The replacement of some part of sulfur into the Ti⁴⁺ TiO₂ lattice distortion and led to the lack of oxygen, improving the visible catalyst activity [133]. Ohno et al. [134] synthesized S-doped TiO₂ which had photo absorption greater than C-doped and N-doped TiO₂ and their absorption depended on the calcination temperature. Their results indicated that S-atoms were incorporated into bulk phase of TiO₂ although but it was not clear whether the S⁴⁺ species were introduced interstitially or at the lattice sites. However, the distortion of the local lattice was an important factor for showing the absorption in the visible region and for the shift of the onset of the absorption edge near 400 nm.

F-doped TiO₂ was investigated and observed high photocatalytic property for the decomposition of acetaldehyde gas under both UV and visible light irradiation [135]. They concluded that the high photocatalytic activity was attributed to several beneficial effects produced by F-doping: enhancement of surface acidity, creation of oxygen vacancies, and increase of active sites. Table 6 shows detailed characteristics of anion-doped TiO₂.

Table 6 Characteristics of anion doped TiO₂

| Anion | Remark |
|-------|----------------------------------------------------------------------------------------------------------------------------------------------------------------------------------------------------------------------------------------------------------------------------------------------------------------------------------------------------------------------------------------------------------------------------------------------------------------------------------------------------------------------------------------------------------------------------------------------------------|
| N | <ul style="list-style-type: none"> - N-doped TiO₂ caused a VB upward shift (narrow band gap and less oxidating holes). N-doped TiO₂ for hydrogen generation was due to electrons for reducing protons and the ability of oxidation did not affect the performance because of more positive of VB level than hydrogen production [136]. - N-doped TiO₂ was effective for methylene blue degradation under visible light [37]. |
| C | <ul style="list-style-type: none"> - C-doped TiO₂ showed photoactivity on degrading 2-propanol under visible light. However, quantum efficiency (0.2%) of C-doped TiO₂ was found inferior than that (2.25%) of N-doped TiO₂ for high photocatalytic activity due to lower quantum efficiency [137]. - Carbon substitution (0.32%) was not effective for the shifting of upper level of the VB towards negative potential during band gap narrowing [138]. |
| S | <ul style="list-style-type: none"> - Ionic radius of S was too large to be incorporated into the lattice of TiO₂ although S-doped TiO₂ resulted in a similar band gap narrowing [37]. - The S ions were replaced with some of the Ti atoms in the form of S⁴⁺ and S-doped TiO₂ showed better degradation of 2-propanol and methylene blue under visible light compared with undoped TiO₂ [134]. - S doping restrained the transformation from anatase to rutile. The band gap shifted from 3 eV to 2.2 eV [137]. |
| P | <ul style="list-style-type: none"> - Dopants (P and C atoms) was less effective as the states were so deep that charge carriers were difficult to be transferred to the surface of TiO₂ [37]. - P-doped TiO₂ in an anatase phase colored yellow exhibited a narrower band gap than pure TiO₂ and an absorption tail in the visible range. This resulted in its effective photocatalytic degradation of 4-chlorophenol under visible-light irradiation [129]. |

F - The disorder layer was recovered by the surface migration of vacancy-type defects and implanted F atoms diffused to the outer surface. The concentration increased with decreasing depths into the surface. The F doping gave rise to a modification of the electronic structure around the CB edge of TiO₂ [135].

3.3 Metal Ion Implantation

Several attempts have been made to deposit metal ions such as Cr, V, Mn, Fe, Ni and Ar in the TiO₂ semiconductor to improve its photocatalytic activity in the visible light region [97,139-141]. High energy transitional metal ions are injected into the lattice of TiO₂ using high energy bombardment to modify the electronic structure of the TiO₂ to make it responsive to the visible light energy. Such modified TiO₂ semiconductor are believed to be one of the most effective visible light photocatalysts and generally referred as second generation photocatalyst [15]. Detailed characteristics of metal ion implantation are shown in Table 7.

Table 7 Characteristics of metal ion implantation on TiO₂

| Metal | Remark |
|------------|--------------------------------------------------------------------------------------------------------------------------------------------------------------------------------------------------------|
| Cr | - Cr deposited TiO ₂ performed very effectively in the decomposition of NO under visible light irradiation [139]. |
| Ag, Mg | - Metal ion-implantation with V, Cr, Mn, Fe and Ni was possible to shift the absorption band toward visible light regions. However, Ag, Mg, or Ti ion-implanted TiO ₂ showed no shift [18]. |
| V, Cr, Mn, | - The effectiveness of the red shift was in the order of V > Cr > Mn > Fe > Ni [97]. |
| Fe, Ni | - Metal ion implanted TiO ₂ (V, Mn and Fe) exhibited high decomposition of propanol to CO ₂ under visible light irradiation [60]. |

3.4 Sensitization

Sensitization is classified into two methods: dye sensitization and composite semiconductor. Dye sensitization is widely applied to utilize visible light for energy conversion and textile wastewater. Table 8 shows commonly used dyes. The dyes have wavelength in the range from 442 nm to 665 nm. Some dyes which have redox property and visible light sensitivity are used in solar cells and photocatalytic reaction. When the dye absorbs visible light, the dye is excited. The dye in the excited state includes lower redox potential than the corresponding ground state. If the redox potential is lower than the CB of TiO₂, an electron is injected from the excited state into the CB. This leads to initiation of photocatalytic reactions. Some dyes (safranin, O/EDTA and T/EDTA) absorb visible light and generate electrons as reducing agents to produce hydrogen [142]. Table 9 shows characteristics of dye sensitization.

Table 8 Dye classification [136]

| Class | Dye |
|-----------|--------------------------------------------------------|
| Thiazines | Thionine, methylene blue, new methylene blue, azure A, |

| | |
|-------------------------------|-------------------------------------------------------------------------------------------------|
| Hiazines | azure B, azure C |
| Phenazines | Toluidine blue |
| Xanthenes | Phenosafranin, safranin-O, safranin-T, neutral red |
| | Fluorescein, erythrosin, erythrosin B, rhodamin B, rose Bengal, pyronine Y, eosin, rhodamine 6G |
| Acridines | Acridine orange, proflavine, acridine yellow |
| Triphenyl methane derivatives | Fusion, crystal violet, malachite green, methylviolet |

Table 9 Characteristics of dye sensitization on TiO₂

| Dye | Remark |
|--------------------|-----------------------------------------------------------------------------------------------------------------------------------------------------------------------------------------------|
| Erosin blue | - Enhancement of hydrogen production rate by different dyes was in the order of erosin blue > rose bengal > Ru(bpy) ₃ ²⁺ > rhodamine B ≈ acriflavin > fluorecein [143]. |
| Azo, naphthol blue | - In aqueous TiO ₂ suspension, azo dyes were effectively degraded by photocatalytic degradation under visible light [144]. |
| black | - Naphthol blue black dyes were decomposed by photosensitized oxidation [145]. |

The approach of semiconductor composition is that when a high band gap semiconductor (TiO₂) is coupled with a low band gap semiconductor (CdS) with more negative CB level, CB electrons can be injected from the low band gap semiconductor to the high band gap semiconductor. Highly dispersed TiO₂ species prepared within zeolite frameworks as well as SiO₂, B₂O₃ and Al₂O₃ matrices showed higher and unique photocatalytic performance as compared with bulk TiO₂ photocatalysts [13]. Particularly, TiO₂ size of less than 10 nm showed significant improvement in photocatalytic reactivity attributed to the quantum size effect. Bo et al. [146] demonstrated that the photocatalytic activity of TiO₂ towards the decomposition of gaseous benzene in a batch reactor was greatly improved by loading TiO₂ on the surface of CeO₂-ZrO₂. The research investigated the effects of three metals doping into Ce_{0.5}Zr_{0.5}O₂ on photocatalytic activity of TiO₂/Ce_{0.45}Zr_{0.45}M_{0.1}OX (M = Y, La, Mn). Doping of metal in TiO₂ increases more crystal defects and oxygen cavities on the surface which captures electron excited from VB to CB thereby impeding the electron-hole pair recombination. Photocatalytic process mainly occurs on the surface of the photocatalyst [146]. Synthesis, characterization and photocatalytic activity of porous manganese oxide doped TiO₂ for the decomposition of toluene reported by [82] which showed better thermal stability and regeneration activity, improved surface area than bulk TiO₂ and require lower catalyst loading.

Conclusions

TiO₂ is one of the most promising semiconductor photocatalyst in the future for environmental applications because of its many excellent properties. Although the main limitation include its poor response to visible natural solar light nevertheless, with more research efforts worldwide, it wont be far when we could one day convert TiO₂ photocatalyst into a very effective photocatalyst for use easily under natural solar light thereby solving many of the photocatalytic limitations. Doping of TiO₂ with other

substances is a very promising method to achieve visible light response TiO₂. The use of TiCl₄ as coagulant in the wastewater treatment serves the dual purpose of sludge management and in producing doped TiO₂ which could open up greater possibilities for next generation of visible light response TiO₂ photocatalyst.

Acknowledgements

This research was supported by a UTS partnership grant and the Center for Photonic Materials and Devices at Chonnam National University (No. R12-2002-054).

References

1. A. Di Paola, E. Garcia-Lopez, S. Ikeda, G. Marci, B. Ohtani, and L. Palmisano, *Catalysis Today*, **75**, 87 (2002).
2. S. Klosek, and D. Raftery, *J. Phys. Chem. B*, **105**, 2815 (2001).
3. O. Diwald, T. L. Thompson, T. Zubkov, E. G. Goralski, S. D. Walck and J. T. Yates, *J. Phys. Chem. B*, **108**, 6004 (2004).
4. R. Bacsa, J. K. Kiwi, T. Ohno, P. Albers, and V. Nadtochenko, *J. Phys. Chem. B: Condens. Matter Mater. Surf. Interfaces Biophys.*, **109**, 5994 (2005).
5. S. Kim, S. J. Hwang, and W. Choi, *J. Phys. Chem. B*, **109**, 24260 (2005).
6. B. Xin, L. Jing, Z. Ren, B. Wang and H. Fu, *J. Phys. Chem. B*, **109**, 2805 (2005).
7. Y. Q. Wang, X. J. Yu, and D. Z. Sun, *Journal of Hazardous Materials*, **144**, 328 (2006).
8. G. Colon, M. Maicu, M. C. Hidalgo and J. A. Navio, *Applied Catalysis B: Environmental*, **67**, 41 (2006).
9. J. Zhao, C. Chen, and W. Ma, *Topics in Catalysis*, **35**, 269 (2005).
10. H. Yamashita, M. Takeuchi, and M. Anpo, Visible-light-sensitive Photocatalysts. *Encyclopedia of Nanoscience and Nanotechnology*. (2004).
11. M. Anpo and M. Takeuchi, *Journal of Catalysis*, **216**, 505 (2003).
12. M. Anpo, *Catalysis Surveys from Japan*, **1**, 169 (1997).
13. M. Anpo, *Bull. Chem. Soc. Jpn.*, **77**, 1427 (2004).
14. D. Chatterjee, and S. Dasgupta., *Journal of Photochemistry and Photobiology C: Photochemistry Reviews*, **186**, (2005).
15. M. Ni, M. K. H. Leung, D. Y. C. Leung, and K. Sumathy, *Renewable and Sustainable Energy Reviews*, **11**, 401 (2007).
16. B. Jelks, *Titanium: its occurrence, chemistry and technology*, New York, Ronald Press, (1966).
17. N. Serpone, and E. Pelizzetti, *Photocatalysis: Fundamentals and Applications*, New York, John Wiley & Sons, (1989).
18. M. Kaneko, I. Okura, *Photocatalysis: Science and Technology*, Springer, Tokyo, 33 (2002).
19. H. K. Shon, S. Vigneswaran, In: S. Kim, J. Cho, G. J. Kim, J. B. Kim, and J. H. Kim, *Environmental Science & Technology*, **41**, 1372 (2007).
20. A. Fujishima, and K. Honda, *Nature*, **238**, 37 (1972).

21. A. Fujishima, T. N. Rao, and D. A. Tryk, *J. Photochem. Photobiol. C: Photo Chem Reviews*, **1**, 1 (2000).
22. B. A. Kennedy, *Surface Mining: 2nd edition*, (1990).
23. T. Brock, M. Grotklaes, Mischke., *European Coatings Handbook*, (2000).
24. B. McKay, *Technological Applications of dispersions*, (1994).
25. R. Noyes, *Pollution prevention technology handbook*. Noyes Publication, Park Ridge, New Jersey, (1993).
26. E. Arpac, F. Sayilkan., M Asiltürk., P Tatar., N. Kiraz and H Sayilkan., *Journal of Hazardous Materials*, **140**, 69(2007).
27. S. G .Lee, S .Lee, Ho-In. Lee, *Applied Catalyst A: General*, **207**, 173 (2001).
28. N.L. Wu, M.S. Lee, *International Journal of Hydrogen Energy*, **29**, 1601 (2004).
29. A. A. Nada, M. H. Barakat, H. A. Hamed, N. R. Mohamed, T. N. Veziroglu, *Int. Journal Hydroden Energy*, **30**,687 (2005).
30. T. Kida, G. Guan, N. Yamada, T. Ma, K. Kimura, and A. Yoshida, *International Journal of Hydrogen Energy* , **29**, 269 (2004).
31. A. Patsoura, D. I. Kondarides and X.E. Verykios, *Catalysis Today*, **124**, 94 (2007).
32. W. Cui, L. Feng, C. Xu, S. Lü and F. Qiu, *Catalysis Communication*, **5**, **533** (2004).
33. K. Sayama, H. Arakawa, *J Photochem Photobiol A: Chem*, **77**, 243 (1994).
34. K. Sayama, H. Arakawa, *J Photochem Photobiol A: Chem*, **94**, 67 (1996).
35. K. Hashimoto, T. Kawai, and T. Sakata, *J. Phys. Chem.*, **88**, 4083 (1984).
36. G. R. Bamwenda, S. Tsubota, T Nakamura, and M. Haaruta, *J. Photochem Photobiol A: Chem*, **89** 177, (1995).
37. R. Asahi, T. Morikawa, T. Ohwaki, K. Aoki and Y .Taga, *Science*, 293, 269 (2001).
38. G. R. Torres, T. Lindgren, J. Lu, CG. Granqvist, SE. Lindquist, *J Phys Chem B*, 108, 5995 (2004).
39. H. Yamashita, M. Harada, J. Misaka, M. Takeuchi, B. Neppolian and M. Anpo, *Catalysis Today*, **84**, 191, (2003).
40. M. Anpo, M. Takeuchi, K. Ikeue, S. Dohshi, *Curr Opin Solid State Mater Sci.*, **6**, 381 (2002).
41. Y. Li, G.Lu, S. Li, *Applied Catalyst A: General*, **214**,179 (2001).
42. X. S. Wu, Z. Ma, Y.N. Qin, X.Z. Qi, and Z.C. Liang, *Wuli Huaxue Xuebao*, **20**, 138 (2004).
43. J. Yuan, M. Chen, J. Shi, W. Shangguan, *International Journal of Hydrogen Energy*, **31**, 1326 (2006).
44. A. J. William, M. B. Daniel, J. A. F. James, E. Boulter, LeAnn, *Air and waste management*, **46**, 891 (1996).
45. Y. Masahiro, K. Yoshiyuki, R. Ariffin, T. Kazunori, K. Shinji, M. Akira, S.H. Lee, Y.K. Hong, S.Y. Shin, *Seidenki Gakkai Koen Ronbunshu*, **1999**, .47 (1999).
46. A. Heller, *Ass. Chem. Res*, **28**,503 (1995)
47. H. Ichiura, T. Kitaoka and H. Tanaka, *Chemosphere*, **50**, 79,(2003).
48. L. Bonafous, *Photo-catalysis Applied to Cementitious Materials. National Science Foundation Workshop on NanoModification of Cementitious Material*, Gainesville, FL. (2006).
49. L. Wang, *Paving out pollution: A common whitener helps to clean the air. Scientific American.com*, (2002).

50. B. Giussani, A concrete Step Toward Cleaner Air. *BusinessWeek.com*, November (2006).
51. E. Povoledo, Church on The Edge of Rome Offers a Solution to Smog. *The New York Times, Europe*, November (2006).
52. S. Hager, and R. Bauer, *chemosphere*, **38**, 1549 (1999).
53. M. C. Hidalgo, S. Sakthivel and D. Bahnemann, *Applied Catalysis A: General*, **277**,183 (2004).
54. D. H. Kim, K.S Lee, Y.S. Kim, Y.C. Chung, and S.J. Kim, *J. Am. Ceram. Soc.*, **89**, 515 (2006).
55. C. H. Ao, S. C. Lee, *Chemical Engineering Science*, **60**, 103 (2005).
56. H. Yanjun, F.Guohui, Y. Quan, Experiment on TiO₂/AC Photocatalysis Technique to Eliminate Toluene in Air Conditioning Systems, ICEBO,china, (2006).
57. R. M. Mohamed, A. A. Ismail, I. Othman and I.A. Ibrahim, *Journal of Molecular Catalysis A: Chemical*, **238**, 151, (2005).
58. F. K. Mohammad, H. Farzana, V. C. H. L. Elena, K. Apostolos, *International Journal of Chemical ReactoE engineering*, **1**,A39,(2003).
59. G. R. Peyton, D.W. DeBerry, Feasibility of Photocatalytic Oxidation for Wastewater Clean-up and Reuse. Report for 4 -31 Mar (1981).
60. H.Yamashita, M. Harada, J. Misaka, M. Takeuchi, K. Ikeue, and M. Anpo, *J. Photochem. Photobiol. A: Chem*, **148**, 257 (2002).
61. Z. Zhonghai, Y. Yuan, F. Yanju, L. Linhong, D. Hongchun, and J. Litong, *Talanta*, **73**, 523 (2007).
62. L. Frazer, *Environmental Health Perspectives*, **109**, 174, (2001).
63. L. Marion, P. Xavier, N. Nikolaus, D. Frank, and N. Reinhard, *Applied Catalysis B: Environmental*, **43**, 205 (2003).
64. K. Hofstadlert and R. Bauer, *Environ. Sci. Technol*, **28**, 670 (1994).
65. M. A. Barakat, Y. T. Chen and C. P. Huang, *Applied Catalysis B: Environmental* , **53**, 13 (2004).
66. J. R. Payne, C. R. Phillips, *Environ. Sci. Technol.*, **19**, 569 (1985).
67. C. Minero, V. Maurino and E. Pelizzetti, *Marine Chemistry*, **58**, 361(1997).
68. M. J. Garcia-Martinez, I.d.Riva, L. Canoira, J.F.Llamas, R. Alcantara, J. L. R.Gallego, *Applied catalyst B: Environmental*, **67**, 279 (2006).
69. A. Heller, M. Nair, L. Davidson, Z. Luo, J.Sshwtzgebel, J. Norrell, J. R. Brock, S. E. Lindquist, J. G. Ekerdt, In: Ollas, D. F., Al-Ekabi, H.(Eds), Photocatalytic Purification and Treatment of water and Air. Elsevier, New York, 139 (1993).
70. R. T. Dabestani, and I. N. Ivanov, *Photochemistry and Photobiology*, **70**, 10 (1999).
71. F. ThomINETTE, J. Verdu, *Oil Chem. Pollut.*, **5**, 333 (1989).
72. P. Litherathy, S. Haider, O. Samhan, G. Morel, *Water Sci.Technol.* **21**, 845 (1989).
73. D. E.Nicodem, C. L. B. Guedes, R. J. Correa, *Mar. Chem*, **63**, 93 (1998).
74. S. Nagata, G. Kondo, Photo-oxidation of Crude Oils, in: Oil Spill Conference, API publication, 617 (1997).
75. R. L. Ziolli, W. F. Jardim, *J. Photochem. Photobiol. A-Chem.*, 155, 243 (2003).
76. A. Fujishima, K. Hashimoto, and T. Watanabe, TiO₂ Photocatalysis: *Fundamentals and Applications*. BKC, Tokyo. (1999).
77. Q. Xie, Z. Xu, C. Shuo, Z. Huimin, C. Jingwen and Z. Yazhi, *Chemosphere*, **60**, 266 (2005).

78. M. Higarashi, W.F. Jardim, *Catalysis Today*, **76**, 201 (2002).
79. Pelizzetti and C. Minero V. Carlin and E. Borgarello, *Chemosphere*, **25**, 343 (1992).
80. M. Hamerski, J. Grzechulska and A.W. Morawski, *Solar Energy*, **66**, 395 (1999).
81. R. Jothiramalingam, and M. K. Wang, *Journal of Hazardous Materials*, In Press, (2007).
82. M. Schiavello (Ed.), *Heterogeneous Photocatalysis*, John Wiley & Sons, New York. (1995).
83. M. Sathish, B. Viswanathan, R. P. Viswanath, and C. S. Gopinath, *Chem. Mater*, **17**, 6349 (2005).
84. J. H. Park, S. Kim, and A. J. Bard, *Nano Letters*, **6**, 24 (2006).
85. C. Y. Wang, C. Y. Liu, X. Zheng, J. Chen and T. Shen, *Colloid Surf. A*, **131**, 271 (1998).
86. V. Subramanian, E. Wolf and P. Kamat, *J. Phys. Chem. B*, **105**, 11493 (2001).
87. Y. Liu, Y. Liu, Q.H. Rong, and Z. Zhang, *Applied surface science*, **220**, 7 (2003)
88. N. Sobana, M. Muruganadham and M. Swaminathan, *Journal of Molecular Catalysis A: Chemical*, **258**, 124 (2006).
89. A. Sclafani, and J. M. Herrmann, *J. Photochem. Photobiol. A Chem*, **113**, 181 (1998).
90. G. Liu, X. Zhang, Y. Xu, X. Niu, L. Zheng and X. Ding, *Chemosphere*, **59** 1367 (2005).
91. J. Liu, Z. Zheng K. Zuo, and Y. Wu, *Journal of Wuhan University of Technology*, **21**, 57 (2006).
92. A. R. Gandhe, and J.B. Fernandes, *J. Solid State Chem.*, **178**, 2953 (2005).
93. P. Bonamali, M. Sharon, and G. Nogami, *Mater. Chem. Phys*, **59** 254 (1999).
94. K. B. Dhanalakshmi, S. Latha, S. Anandan, and P. Maruthamuthu, *Int. J Hydrogen Energy*, **26**, 669 (2001).
95. M.G. Kang, N. G. Park, Y. J. Park, K. S. Ry, and S. H. Chang, *Sol. Energy Mater. Sol. Cells*, **75**, 475 (2003).
96. J. R. Sambrano, G. F. Nobrega, C. A. Taft, J. Andres, and A. Beltran, *Surface Science*, **580**, 71 (2005).
97. M. Anpo, and M. Takeuchi, *Journal of Catalysis*, **216**, 505 (2003).
98. H. E. Chao, Y. U. Yun, F. Xing, A. Larbot., *Journal of European ceramic society*, **23**, 1457 (2003).
99. A. V. Rupa, D. Manikandan, D. Divakar, and T. Sivakumar, *Journal of Hazardous Materials*, In Press, (2007).
100. R. S. Sonawane, and M. K. Dongare, *Journal of Molecular Catalysis A: Chemical*, **243**, 68 (2006).
101. A. Mirescu, H. Berndt, A. Martin, and U. Prüße, *Applied Catalysis A: General*, **317**, 204 (2007).
102. S. Sakthivel, M. Janczarek, and H. Kisch, *J. Phys. Chem. B*, **108**, 19384 (2004).
103. K. Kontapakdee, J. Panpranot, and P. Praserttham. *Catalysis Communications*, In Press, (2007)
104. T. Sreethawong, and S. Yoshikawa, *Catalysis Communications*, **6**, 661 (2005).
105. E.S. Bardos, H. Czili, and A. Horvath, *J Photochem Photobiol A: Chem*, **154**, 195 (2003).
106. W. K. Wong, and M. A. Malati, *Solar Energy*, **36**, 163 (1986)

107. J. Zhou, M. Takeuchi, A.K. Ray, M. Anpo, and X.S. Zhao, *Journal of Colloid and Interface Science*, **311**, 497 (2007).
108. S. Karvinen, *Solid State Sciences*, **5**, 811 (2003).
109. W. Y. Teoh, R. Amal, L. Madler and S. E. Pratsinis, *Catalysis Today*, **120**, 203 (2007).
110. E. Piera, M. I. Tejedor- Tejedor, M. E. Zorn, and M. A. Anderson, *Applied Catalysis B: Environmental*, **4**, 671 (2003)
111. M.I. Litter, *Appl Catal B: Environ*, **23**, 89 (1999).
112. W.Y. Choi, A. Termin, M.R. Hoffmann, *J. Phys. Chem.*, **84**, 13669 (1994).
113. S. T. Martin, C. L. Morrison, and M. R. Hoffmann, *J. Phys. Chem*, **98**, 13695 (1994).
114. D. S. Muggli, S. A. Larson, and J. L. Falconer, *J. Phys. Chem.*, **100**, 15886 (1996).
115. M. Anpo, Y. Ichihashi, M. Takeuchi, and H. Yamashita., *Res. Chem. Intermed*, **24** 143, (1998).
116. S. J. Hwang, and D. Raftery, *Catalysis Today*, **49**, 35 (1999).
117. S. Pilkenton, S.J. Hwang, and D. Raftery, *J. Phys. Chem. B*, **103**, 11152 (1999).
118. G. L. Zhao, H. Kozuka, H. Lin, and T. Yoko, *Thin Solid Films*, **339**, 123 (1999).
119. Y. Wang, H. Cheng, L. Zhang, Y. Hao, J. Ma, B. Xu, and W. Li, *Journal of Molecular Catalysis A: Chemical*, **151**, 205 (2000).
120. D. S. Hwang, N. H. Lee, D.Y. Lee, J. S. Song, S. H. Shin, and S. J. Kim, *Smart Mater. Struct.*, **15**, S74-S80 (2006).
121. U. Diebold, *Surf. Sci. Rep*, **48**, 53 (2003).
122. C. Li, L. Shi, D. Xie, and H. Du, *Journal of Non-Crystalline Solids*, **352**, 4128 (2006).
123. B.Y. Lee, S.H. Park, M. Kang, S.C. Lee, and S.J. Choung, *Applied Catalysis A: General*, **253**, 371 (2003).
124. Y. J. Choi, Z. Seeley, A. Bandyopadhyay, S. Bose and S. A. Akbar., *Sensors and Actuators B Chemical*, **124**, 111 (2007).
125. J.C.S. Wu, and C.H. Chen, *J. Photochem. Photobiol. A: Chem.*, **163**, 509 (2004).
126. A. W. Xu, Y. Gao, and H.Q. Liu, *J Catal*, **207**, 151 (2002).
127. S. Sato, *Chemical Physics Letters*, **123**, 126 (1986).
128. H. Irie, Y. Watanabe, and K. Hashimoto, *J. Phys. Chem. B*, **107**, 5483 (2003).
129. Z. Lin, A. Orlov, R.M. Lambert, and M.C. Payne, *J. Phys. Chem. B*, **109**, 20948 (2005).
130. C. D. Valentin, G. Pacchioni, and A. Selloni, *Phys. Rev. B*, **70**, 085116 (2004).
131. K. Yang, Y. Dai, B. Huang, and S. Han, *J. Phys. Chem. B*, **110**, 24011 (2006).
132. H. Irie, S. Washizuka, and K. Hashimoto, *Thin Solid Films*, **510**, 21 (2006).
133. Z. Wushu, C.S.Q. Tang, and L. Ying, *China Nonferrous Metals Journal*, **0907** (2006).
134. T. Ohno, M. Akiyoshi, T. Umebayashi, K. Asai, T. Mitsui, and M. Matsumura, *Appl. Catal. A: Gen.*, **265**, 115 (2004).
135. D. Li, H. Haneda, S. Hishita, N. Ohashi and N. K. Labhsetwar, *Journal of Fluorine chemistry*, **126**, 69 (2005).
136. M. Mrowetz, W. Balcerski, A. J. Colussi, and M. R. Hoffmann, *J. Phys. Chem. B*, **108**, 17269 (2004).

137. H. Irie, Y. Watanabe, and K. Hashimoto, *Chem. Lett.*, **32**, 772 (2003a).
138. H. Irie, Y. Watanabe and K. Hashimoto, *J. Phys. Chem. B*, **107**, 5483 (2003b).
139. M. Takeuchi, H. Yamashita, M. Matsuoka, M. Anpo, T. Hirao, and N.E.A. Itoh, *Catal. Lett.*, **67**, 135 (2000).
140. M. Anpo, S. Kishiguchi, Y. Ichihashi, M. Takeuchi, H Yamashita, and K. Ikeue, *Res Chem Intermed*, **27**, 459,(2001).
141. A. Tsujiko, K. Kajiyama, M. Kanaya, K. Murakoshi, and Y. Nakato, *Chemical Society of Japan*, **76**, 1285 (2003).
142. Z.C. Bi, and H.T. Tien., *Int. J. Hydrogen Energy*, **9**, 717,(1984).
143. K. Gurunathan, P. Maruthamuthu and V.C. Sastri, *Int. J. Hydrogen Energy.*, **22**, 57 (1997).
144. M. Styliidi, D.I. Kondarides, and X.E. Verykios, *Appl. Catal. B: Environ.* **47**, 189 (2004).
145. K. Vinodgopal, and P.V. Kamat, *Environ. Sci. Technol.*, **29**, 841 (1995).
146. Z. J. Bo, Lintao, G. Maochu, W. J. Li, L. Z. Min, Z. Ming and Y. Chen, *J. of Hazard. Mater.*, **143** ,516 (2006).